

## Color temperature measurement in laser-driven shock waves

T. A. Hall,<sup>1</sup> A. Benuzzi,<sup>2</sup> D. Batani,<sup>3</sup> D. Beretta,<sup>3</sup> S. Bossi,<sup>3</sup> B. Faral,<sup>2</sup> M. Koenig,<sup>2</sup> J. Krishnan,<sup>2</sup> Th. Löwer,<sup>4</sup> and M. Mahdih<sup>1</sup>

<sup>1</sup>*Department of Physics, University of Essex, Wivenhoe Park, Colchester CO4 3SQ, United Kingdom*

<sup>2</sup>*Laboratoire pour l'Utilisation des Lasers Intenses, CNRS, Ecole Polytechnique, 91128 Palaiseau, France*

<sup>3</sup>*Dipartimento di Fisica dell'Università degli Studi di Milano and Istituto Nazionale di Fisica della Materia, Unità di Milano, via Celoria 16, 20133 Milano, Italy*

<sup>4</sup>*Max Planck Institut für Quantenoptik, D-85748 Garching, Germany*

(Received 5 November 1996)

A simultaneous measurement of color temperature and shock velocity in laser-driven shocks is presented. The color temperature was measured from the target rear side emissivity, and the shock velocity by using stepped targets. A very good planarity of the shock was ensured by the phase zone plate smoothing technique. A simple model of the shock luminosity has been developed in order to estimate the shock temperature from the experimental rear side emissivity. Results have been compared to temperatures obtained from the shock velocity for a material of a known equation of state. [S1063-651X(97)50806-3]

PACS number(s): 52.35.Tc, 62.50.+p

### I. INTRODUCTION

Knowledge of the equation of state (EOS) of strongly compressed materials is of great important in inertial confinement fusion (ICF) and planetary physics research fields. The EOS in the megabar range can be determined using laser-driven shocks produced by high power lasers. Recently [1,2], the possibility of achieving *relative* EOS measurements with a good precision has been demonstrated in the pressure domain previously achieved only in nuclear tests. *Absolute* EOS measurements are much more difficult to perform, since they require the simultaneous measurement of two shock parameters. The shock velocity  $D$  is a relatively easy quantity to measure with a good precision. In earlier experiments [3], the feasibility of simultaneous measurement of  $D$  and the fluid velocity  $U$  has been demonstrated, provided that a very high-power laser is available. More recently, the measurement of these two quantities has been performed in shocked liquid deuterium [4].

Another quantity which can be measured (with optical techniques) is the shock temperature  $T_s$ . This measurement would also provide valuable additional information on the thermodynamic properties of the material. It must be pointed out that the temperature is the most uncertain quantity in EOS physics, in the sense that it is the parameter on which the discrepancy between currently available EOS models [such as the SESAME library [5] and the quotidian equation of state (QEOS) model [6]] is the most important. Direct measurements of  $T_s$  can be easily performed with materials that are transparent in their initial state [7]. In the case of an opaque material, such measurements could only be made at the time the shock arrives at the solid-vacuum interface, before the plasma expands into the vacuum. The finite temporal resolution of the instruments makes such direct measurements of  $T_s$  impossible, and leads to the measurement of the properties of the expanding plasma instead. In this case a proper model of plasma expansion must be used in order to deduce material parameters at shock breakthrough from those measured at later times.

The first measurement of the rear surface temperature was made by McLean *et al.* [8] in order to study the mechanisms of energy transport in the dense target material. A more recent work in this direction was made by Ng *et al.* [9]. In their experiment, spectral and brightness temperatures were measured. Even though such results were encouraging, they were affected by intrinsic limitations. First, the brightness temperature determination requires an absolute calibration of the complete optical system, which is a difficult measurement. Indeed such a calibration induced an error of  $\pm 50\%$  in their results. In their experiments, the spectral temperature measurement technique precludes a simultaneous measurement of the quality of the shock (i.e., the planarity and hence the uniformity of parameters) and also a measurement of the shock velocity on each shot. Therefore, they were not able to verify on each shot the consistency of the spectral and brightness temperatures with the other shock parameters.

In this paper we present the first simultaneous measurements of target rear side color temperature and shock velocity. Very planar shock fronts have been obtained using the phase zone plates (PZP) optical-smoothing technique [10]. The color temperature was determined by recording the space-time-resolved rear surface emissivity in two different spectral regions on the same detector. The imaging technique allowed us to check the shock quality shot by shot. From a simple model (presented in Sec. III) which calculates the rear surface emissions, we obtained an estimate of the shock temperature, noted  $T_s^m$ , where the superscript  $m$  stands for "model." From a precise measurement of the shock velocity using stepped targets and knowing the EOS, it is possible to deduce the actual shock temperature  $T_s^{\text{EOS}}$ . It is for this reason that we used Al targets, of which the EOS is well known (e.g., from the SESAME library) in the range of pressures investigated in this paper ( $P \leq 12$  megabar). The value of the shock temperature  $T_s^{\text{EOS}}$  can then be used to check the validity of  $T_s^m$  as an estimation of the shock temperature.

### II. PRINCIPLE OF THE EXPERIMENT AND SETUP

The experiment was performed at the LULI laboratory. The Al targets were irradiated with a  $\lambda=0.53 \mu\text{m}$  Gaussian

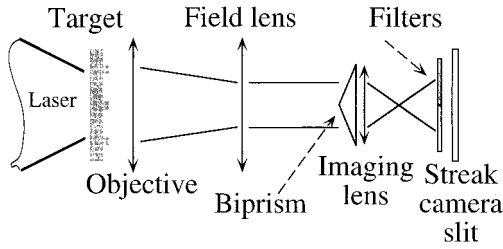


FIG. 1. Schematic arrangement of the setup. A field lens has been used in the imaging system to eliminate the vignetting effects caused by the aperture of the objective.

laser pulse with a full width at half maximum (FWHM) approximately equal to 600 ps. The laser pulse was focused by a  $f = 50$  cm lens onto the target. The characteristics of our optical system (PZP plus focusing lens) were such that a focal spot of  $\approx 350\text{-}\mu\text{m}$  FWHM with a flat region of  $\approx 200\text{ }\mu\text{m}$  was produced. Spatially averaged intensities between  $3 \times 10^{13}$  and  $10^{14}$  W/cm<sup>2</sup> were obtained, depending on the number of laser beams we used. An optical system made of an objective, two lenses and a biprism allowed the image of the target rear face to be split into two onto the slit of a visible streak camera. A different colored filter was then used in front of each image. In this way, we measured on each shot the emissivities  $I_r$  and  $I_b$  of the red and blue regions of the visible spectrum, respectively. The streak camera temporal resolution was of  $\approx 10$  ps. The imaging system magnification was  $M = 10$ , resulting in a spatial resolution of  $10\text{ }\mu\text{m}$  at the target plane. The correct alignment of the biprism was very critical for the experiment. In order to check precisely this alignment, during the experiment we recorded at regular intervals the double image (without filters) of a transparent target positioned in the center of the chamber with the streak camera in static mode. We then verified that the intensities in the two images were well balanced. A schematic arrangement of the imaging system is shown in Fig. 1.

The convolution of the blue transmission filter with the streak camera spectral response,  $\Phi_b(\lambda)$  is a curve characterized by a maximum of 20% transmission around 400 nm. For the red ‘‘channel,’’ the curve  $\Phi_r(\lambda)$  has a maximum of 35% transmission around 600 nm. The filter transmission functions have been measured with a spectrophotometer. The streak camera has been spectrally calibrated *in situ* by using a spectrometer [11]. In order to have a good precision on the time scale, we have also performed the temporal calibration of the streak camera by using the ultra-short laser pulse ( $\approx 250$  fs) at LULI [11]. We have verified that, for the optics used, the time delay between  $I_r$  and  $I_b$  due to the group velocity dispersion is still shorter than our time resolution.

From the ratio  $I_r/I_b$  we could then deduce the color temperature  $T_c$  which is defined [12] as the temperature of a perfect blackbody, which would yield a ratio of brightness in two spectral regions equal to the experimentally measured ratio. The color temperature is expected to be different from the real one because the emission is not a perfect blackbody. In addition, absorption between the point of emission and the observer will differentially affect the values of  $I_r$  and  $I_b$ . By taking into account the transmission function of the filters we used, we deduced the curve  $T_c(I_r/I_b)$ . The ratio of the intensities is insensitive to changes in temperature for tempera-

tures above  $\approx 6$  eV (this corresponds to  $I_r/I_b$  below  $\approx 0.6$ ). For such values of temperature the maximum of blackbody emission lies in the XUV region, and hence the visible region is in the tail of the curve. This implies that a small variation of the measured ratio of  $I_r/I_b$  corresponds to a very large change in temperature. For temperatures below  $\approx 1$  eV ( $I_r/I_b$  above  $\approx 1.5$ ), we have the opposite behavior: the temperature is not very sensitive to a variation of the ratio  $I_r/I_b$ . Therefore, in our case, the color temperature diagnostic can be reasonably applied in the 1–6 eV region (corresponding to a pressure range  $2 < P < 12$  megabar for Al). Because of the finite streak camera resolution time, the color temperature measurement at the shock breakout corresponds to a time when the plasma is already expanding into the vacuum, and not to the instant of shock breakout. Hence the measured temperature gives a lower bound for the shock temperature. In fact, the expanding material forms a cool, absorbing layer obscuring the higher-temperature material behind it.

In order to measure the shock velocity  $D$ , we focused the smoothed laser beam using the PZP technique on to a aluminum grid target (see Fig. 1). The high quality of the shocks that were produced and the use of grid targets allowed a very precise determination of the shock velocity shot by shot [1]. The shock velocity is obtained by measuring the shock breakthrough times from both the base and the step. The base thickness of the targets were in the range of 12–15  $\mu\text{m}$ , while the step thicknesses were 5–6  $\mu\text{m}$  in addition. The choice of targets thicknesses was suggested by simulations, performed with the one-dimensional hydrodynamic code FILM developed at Ecole Polytechnique, under the condition of ensuring constant shock pressure in the steps. The spacing between the steps was  $\approx 140\text{ }\mu\text{m}$ , while the width of the steps was  $\approx 40\text{ }\mu\text{m}$ . Therefore, such a geometry together with our focal spot dimension ensured there was always one step within the flat region of the focal spot.

### III. DATA ANALYSIS

In order to achieve good experimental results, it is necessary to produce high-quality shocks. Indeed, only if high-quality shocks are obtained is it possible to ensure uniformity of plasma parameters and hence to measure the shock parameters precisely. In order to find the optimal position for PZP [10] and to check the shock quality, simple aluminum targets were used. Once the planarity of the shock was established, we used grid targets for the shock velocity measurements. A typical image obtained is shown in Fig. 2. It can be seen that the shock is perfectly planar on a dimension of  $\approx 200\text{ }\mu\text{m}$  which corresponds to the focal spot flat region. The time-resolved blue and red emissivities are shown in Fig. 3(a). First, as mentioned in previous papers [13,14], we note that the shapes of the two signals are typical of negligible pre-heating effects. Then we observe that the two emissivities have different decay times. This happens because, at early times, the temperature is a few eV, and hence the maximum of the emissivity is in the UV region, while at later times the plasma cools down and the maximum moves toward lower energies. The color temperature, corresponding to the emissivities of Fig. 3(a), is shown in Fig. 3(b), as a function of

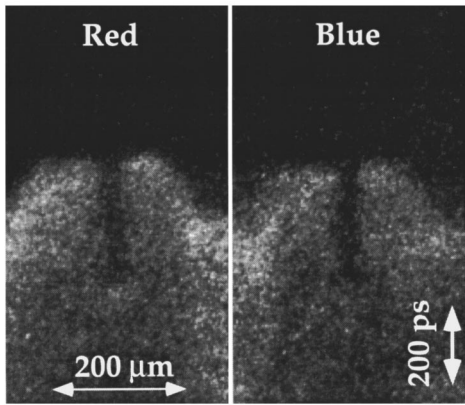


FIG. 2. Typical streak camera record of the “red” and “blue” spectral light emitted by the rear side of a grid aluminum target. The base thickness is  $13.55 \mu\text{m}$ , and the step thickness is  $5.7 \mu\text{m}$ .

time. It can be seen that the plasma cooling yields a decrease of  $T_c$  with time.

When a shock wave reaches the interface between solid and vacuum the surface material begins to expand [12]. In our case, the shock wave is so strong that the metal is completely vaporized on unloading and expands in a gas and/or plasma phase. The region from which the radiation is emitted becomes larger with time. At the same time the material cools down and the emission decays. In order to evaluate the shock temperature, we developed a simple model which reproduces the blue and red emission. This model is based on the following.

(i) The usual assumption is that the hydrodynamic expansion is an isentropic self-similar rarefaction wave [12]. We preferred such a description instead of those given by usual Lagrangian hydrodynamic codes, because the sensitivity of the cell size prevents a reliable description of rear side expansion. Recently [15,16], it was pointed out that the expansion

should be considered as isothermal in the first  $\approx 5$  ps after the shock breakthrough, and becomes isentropic only after this characteristic time. We did not take this effect into account, since it takes place on a time scale shorter than our temporal resolution.

(ii) The assumption of the Kramers-Unsöld opacity, as suggested by Ref. [12] for the absorption of visible light in metallic vapors. Such an absorption coefficient accounts for free-free and bound-free transitions involving highly excited states of hydrogenlike atoms. This formula accurately describes the absorption in the low-density region, while it does not apply in high-density regions. The problem of opacity calculations for the visible light in highly compressed ( $\approx 1-3$  times the solid density) and cold matter (approximately equal to a few eV) is a very difficult problem which has not yet been solved. As far as we are aware, all the shock visible luminosity calculations performed so far have used a power law for the opacities (Kramers-Unsöld or the free-free absorption formula) [14,17,18]. In Ref. [17], the authors used also Rosseland frequency-averaged opacities from the SESAME library, which is rather questionable, since frequency averaging leads to an important overestimation of the luminosity.

(iii) The use of More’s [19] formula for the mean ionic charge, which is based on the Thomas-Fermi model, gives a reliable value for degenerate plasmas.

The calculation of  $I_r$  and  $I_b$  has been undertaken using the hypothesis of local thermal equilibrium (in our case the thermalization characteristic times are smaller than the hydrodynamic characteristic times). Hence at each time we used the solution of the transfer radiation equation [12].

We noticed that at early times ( $\approx 10-50$  ps after the shock breakthrough) the radiation can come from regions slightly overcritical (at most  $\approx 0.1 \mu\text{m}$  beyond the critical layer position) since a screening layer has not yet completely developed. However, in our calculations we did not have to take into account any particular effects near the critical layer. Indeed the sharp cutoff at  $\omega = \omega_p$  occurs at low pressures only (when  $\nu_{ei}/\omega \leq 1$ ;  $\nu_{ei}$  is the electron-ion collision frequency,  $\omega$  is the light frequency, and  $\omega_p$  the plasma frequency) and becomes less and less distinct as collisional damping increases [20]. At early times, the plasma has not yet expanded and we are clearly in the opposite regime ( $\nu_{ei}/\omega \gg 1$ ) [16].

We determined  $T_s^m$  by changing its value and the adiabatic coefficient  $\gamma$  in the self-similar expanding profiles, until we found the best interpolation of our experimental curves. We varied  $\gamma$  in the range  $\approx 1.2-1.7$ , as expected in rarefaction after a strong shock [14]. The results are shown in Fig. 4, where the color temperatures  $T_c$  (at the shock breakthrough time) and the shock temperatures  $T_s^m$  are compared with the shock temperatures  $T_s^{\text{EOS}}$  given by the SESAME equation of state. The calculated values of the shock temperature  $T_s^m$  are not too far from those obtained from the SESAME EOS. Part of the difference may be due to a poor description of plasma opacities. As expected, the color temperatures  $T_c$  are an underestimation of the shock temperatures  $T_s^{\text{EOS}}$  due to the rear surface expansion. The error bar for the shock velocity measurement ( $\pm 4\%$ ) was determined by considering the uncertainties on: the step thicknesses, the shock breakthrough time, and the streak camera sweep speed. The error bar for

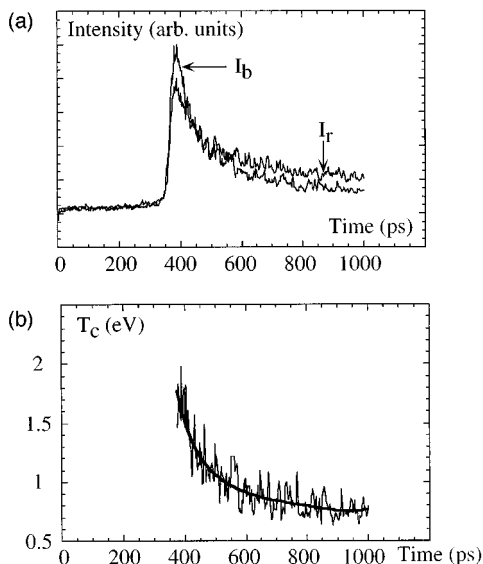


FIG. 3. (a) Emissivities in the red and blue regions of the shocked target rear side as a function of time. (b) Color temperature as a function of time deduced from the ratio of the two emissivities. The solid line represents the best fit.

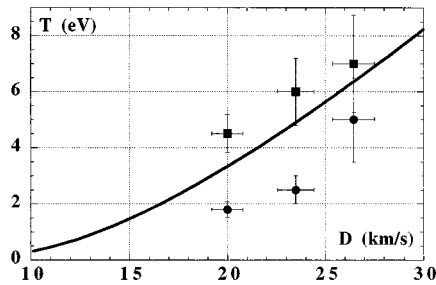


FIG. 4. Aluminum shock temperature  $T_s$  vs shock velocity  $D$ . The solid line corresponds to  $T_s^{\text{EOS}}$  given by SESAME EOS, the solid circles to color temperature  $T_c$  measurements and the solid squares to the shock temperature  $T_s^m$  obtained by the model.

the color temperature measurement was determined by taking into account the uncertainty that comes principally from an imperfect alignment of the optical system. Obviously, the error in the ratio  $I_r/I_b$  implies an error in  $T_c$  which depends on the behavior of the function  $T_c(I_r/I_b)$  (cf. Sec. II). According to the previous explanation, the error increases considerably with the shock strength. The error varies in the range  $\pm 15\text{--}20\%$  for the two points at lower temperatures,

while the error for the third point is more important ( $\pm 30\%$ ), since it lies near the limit of the diagnostic applicability (cf. Sec. II).

#### IV. CONCLUSIONS

In this paper the efficacy of a color temperature measurement as diagnostic of shock breakout was demonstrated for the first time, to our knowledge. The color temperature and shock velocity were measured on the same laser shot. By using a reference material (Al), we obtained a direct comparison between the shock temperature deduced from the SESAME EOS and the color temperature. Using a simple model for the target rear side emissivity, we obtained an independent estimation of the shock temperature. If, in the future, accurate opacity data are improved, the method presented here would provide a more precise shock temperature determination in the 1–6 eV temperature regime.

#### ACKNOWLEDGMENTS

This work was supported by the EU Human Capital and Mobility program under Contract Nos. CHRX-CT93-0338 and ERB-CHGE-CT93-0046. We wish to thank S. Hüller and Ph. Mounaix for useful discussions.

- 
- [1] M. Koenig *et al.*, Phys. Rev. Lett. **74**, 2260 (1995).
  - [2] A. Benuzzi *et al.*, Phys. Rev. E **54**, 2162 (1996).
  - [3] B. A. Hammel *et al.*, Phys. Fluids **B5**, 2259 (1993).
  - [4] L. Da Silva *et al.*, Phys. Rev. Lett. **78**, 483 (1997).
  - [5] SESAME Report on the Los Alamos Equation-of-State Library, Report No. LALP-83-4 (T4 Group LANL, Los Alamos, 1983).
  - [6] R. M. More *et al.*, Phys. Fluids **31**, 3059 (1988).
  - [7] Ya. B. Zel'dovich *et al.*, Dokl. Akad. Nauk. SSSR **122**, 48 (1958).
  - [8] E. McLean *et al.*, Phys. Rev. Lett. **45**, 1246 (1980).
  - [9] A. Ng *et al.*, Phys. Rev. Lett. **54**, 2604 (1985).
  - [10] M. Koenig *et al.*, Phys. Rev. E **50**, R3314 (1994).
  - [11] A. Benuzzi *et al.*, LULI Laboratory Report No. 283, 1995 (unpublished).
  - [12] Ya. B. Zel'dovich and Yu. P. Raizer, *Physics of Shock Waves and High Temperature Hydrodynamic Phenomena* (Academic, New York, 1967).
  - [13] Th. Löwer *et al.*, Phys. Rev. Lett. **72**, 3186 (1994).
  - [14] S. Hüller *et al.*, Gesellschaft für Schwerionenforschung, Report No. GSI-94, Darmstadt, 1994 (unpublished).
  - [15] D. Parfeniuk *et al.*, Can. J. Phys. **66**, 662 (1988).
  - [16] P. Celliers and A. Ng, Phys. Rev. E **47**, 3547 (1993).
  - [17] L. Da Silva *et al.*, J. Appl. Phys. **58**, 3634 (1985).
  - [18] M. Mahdiah and T. Hall, Laser Part. Beams **14**, 149 (1996).
  - [19] R. M. More, *Applied Atomic Collision Physics* (Academic Press, New York, 1982).
  - [20] G. Bekefi, *Radiation Processes in Plasmas* (Wiley, New York, 1966).